https://doi.org/10.5194/tc-2021-181
Preprint. Discussion started: 14 July 2021

The Cryosphere Discussions

Brief communication: ICESat-2 reveals seasonal thickness change patterns of Greenland Ice Sheet outlet glaciers for the first time

Christian J. Taubenberger[1,2], Denis Felikson[1,3], Thomas Neumann[1]

[1]Cryospheric Sciences Laboratory, NASA Goddard Space Flight Center, Greenbelt, Maryland, 20771, United States of America

[2]Atmospheric, Oceanic & Earth Sciences Dept., George Mason University, Fairfax, Virginia, 22030, United States of America

[3]Goddard Earth Sciences Technology and Research Studies and Investigations, Universities Space Research Association, Columbia, MD 21046, United States of America

Correspondence to: Christian J. Taubenberger (ctaubenberger@gmail.com)

Abstract

Dynamic changes of marine-terminating outlet glaciers are projected to be responsible for about half of future ice loss from the Greenland Ice Sheet. However, we lack a unified, process-based understanding that can explain the observed dynamic changes of all outlet glaciers. Many glaciers undergo seasonal dynamic thickness changes and classifying the patterns of seasonal thickness change can improve our understanding of the processes that drive glacier behavior. The Ice, Cloud and land Elevation Satellite (ICESat-2) provides the first space-based, seasonally repeating altimetry measurements of the ice sheets, allowing us to quantify near-termini seasonal dynamic thickness patterns of 34 outlet glaciers around the Greenland Ice Sheet. We classify the glaciers into seven common patterns of seasonal thickness change over a two-year period from 2019 to 2020. We find small groupings of neighboring glaciers with similar seasonal thickness change patterns but, within larger sectors of the ice sheet, seasonal thickness change patterns are heterogeneous. Comparing the seasonal thickness changes to average glacier ice flow speeds, we find that faster glaciers typically undergo patterns of spring and summer dynamic thickening, while slower glaciers exhibit a variety of thickness change patterns. Future studies can build upon our results by comparing seasonal dynamic thickness changes with external forcings, such as ocean temperature and meltwater runoff, and with other dynamic variables such as seasonal glacier velocity and terminus position changes.

1 Introduction

Understanding the complex nature of Earth's ice sheets is of critical importance as they have undergone dynamic changes in recent decades (Church et al., 2013; Oppenheimer et al., 2019). Greenland Ice Sheet (GrIS) marine-terminating outlet glaciers, which drive dynamic ice mass change, are projected to account for 50 ± 20% of total mass loss over the 21st century (Choi et al., 2021). While multi-year and decadal changes of ice sheet discharge via outlet glaciers have been studied before (Mouginot et al., 2019), patterns of seasonal thickness change have not yet been studied for a representative sample of GrIS

https://doi.org/10.5194/tc-2021-181
Preprint. Discussion started: 14 July 2021

outlet glaciers. Outlet glaciers exhibit seasonal fluctuations in velocity with distinct patterns (Moon et al., 2014; Vijay et al., 2019) but the lack of seasonal thickness change measurements contributes to a lack of understanding of what processes control glacier dynamics on seasonal time scales. Seasonal thickness changes of outlet glaciers are driven by both external forcings (e.g., precipitation, evaporation, runoff, terminus melt) and internal glacier dynamics (e.g., subglacial and englacial hydrology, terminus calving) and classifying their patterns of seasonal thickness change is the first step towards a more holistic understanding of the processes that control them. Here, we measure dynamic ice sheet thickness near the termini of 34 GrIS outlet glaciers at seasonal resolution for the first time using the ATL06 land ice along-track altimetry dataset from the Ice, Cloud and land Elevation Satellite-2 (ICESat-2; Markus et al, 2017; Neumann et al, 2019). Large scale observational studies such as this allow for smaller, less studied, glaciers to be observed at the same time as more well-studied glaciers and comparisons to be drawn into how these lesser-known glaciers compare with the seasonal thinning of larger glaciers, which is critical for better understanding the drivers of dynamic change in a changing climate across all outlet glaciers. We use each glacier's temporal pattern of seasonal dynamic thickness changes to group glaciers into 7 distinct patterns over 2019 and 2020. Given that we present just one to two years of data, our results are not intended to definitively characterize these glaciers but, rather, to present a method for quantifying seasonal dynamic thickness changes and to highlight the heterogeneity exhibited by these glaciers over the study time period. We discuss ways in which future work could build on our results in Section 4.

2 Data and methods

We used three data sources within this study: (1) The ATLAS/ICESat-2 L3A Land Ice Height, Version 3 (ATL06) data product, acquired by the Advanced Topographic Laser Altimeter System (ATLAS) instrument on board the ICESat-2 observatory, which provides geolocated measurements of land-ice surface heights (Smith et al., 2019); (2) Making Earth System Data Records for Use in Research Environments (MEaSUREs) glacier termini dataset of annual Greenland outlet glacier locations from Synthetic Aperture Radar (SAR) mosaics and Landsat 8 OLI imagery, version 1 (Joughin et al., 2015), from which we use outlet glacier locations and identifier (ID) numbers; (3) Greenland Ice Mapping Project Digital Elevation Model (GIMP DEM; Howat et al, 2014), a digital surface elevation model of the GrIS that we used as a reference height dataset to remove along- and across-track surface slopes from the ATL06 measurements.

ATL06 provides measurements of ice sheet surface elevation at an along-track spatial resolution of 20 m, which allows for ample spatial sampling of the fast-flowing, dynamic portions of GrIS outlet glaciers (Smith et al., 2020). We use elevation data (h_li) retrieved from all six ATLAS ground tracks to achieve the highest quantity of data available. ICESat-2 has a repeat cycle of 91 days, allowing for sufficient temporal sampling to measure seasonal changes of glaciers, although we do not receive data from every satellite pass due to cloud interference. We filter out poor quality ATL06 height data using the ATL06 quality summary flag (atl06_quality_summary), keeping only data for which the flag is set to zero.

The MEaSUREs glacier termini dataset contains locations for 238 glaciers across the GrIS, as well as an ID number (Joughin et al, 2015). We selected 65 glaciers from the MEaSUREs dataset due to their spatial distribution across several GrIS

https://doi.org/10.5194/tc-2021-181
Preprint. Discussion started: 14 July 2021

regions and range of average ice discharges between 68 m/yr and 8141 m/yr (Rignot and Mouginot, 2012). The 65 glaciers chosen for this study also correspond to the glaciers for which a dense record of terminus positions has been generated by the Calving Front Machine (CALFIN; Cheng, 2020). The CALFIN dataset is currently the only pan-Greenland dataset of seasonal terminus positions. Although we do not use this dataset in this study, our selection of glaciers will enable comparisons of seasonal thickness change with seasonal terminus position in future studies. We define glacier seasons by three-month periods of winter (Dec-Jan-Feb), spring (Mar-Apr-May), summer (Jun-Jul-Aug), and autumn (Sep-Oct-Nov). We removed glaciers that do not contain a full year (4 seasons) of ICESat-2 data from either 2019 or 2020, reducing the number of glaciers categorized to 42 (listed in supplementary spreadsheet).

To collect ATL06 measurements representative of near-terminus glacier thickness change, we created a 2 km x 2 km bounding box for each glacier, centered on each glacier's location in the MEaSUREs dataset, within which we aggregated ATL06 data. We manually adjusted the MEaSUREs glacier locations slightly to ensure between one and three ICESat-2 repeat ground tracks intersect each box but we kept each bounding box within 10km of the terminus for each glacier. The $4km^2$ bounding box was chosen as an arbitrary size, however it was kept to this size as a larger box may include data off the main fast flowing section of the outlet glacier.

The GIMP DEM represents the mean ice sheet surface elevation between 2003 and 2009 (Howat et al, 2014). The elevation data has a 90 m spatial resolution and is used as the reference ice sheet surface elevation to account for the surface slope of the glaciers. Because the repeating passes of ICESat-2 do not exactly survey the same location on the surface of the ice sheet, ATL06 measurements from season to season are affected by both the vertical component of surface elevation change as well as differences in surface elevation due to surface slope. To account for this, we sampled the GIMP DEM at each ATL06 measurement and subtracted the GIMP DEM elevation from each ATL06 surface elevation measurement. This effectively changes the datum of the ATL06 measurements to the GIMP DEM, thereby accounting for the surface slope of the ice sheet within our bounding boxes, leaving just the vertical component of surface elevation change.

We use the ATL06 data within each bounding box, a surface mass balance model, and a firn model to calculate each glacier's dynamic thickness change from season to season. For each glacier, we calculate the surface elevation change (dH) between ICESat-2 observations and the GIMP DEM. We then calculated the seasonal dynamic dH as the mean of the dHs within each bounding box for each year and season, and we subtracted the surface elevation change due to changes in surface mass balance (SMB) and firn air content changes using output from the Community Firn Model (CFM; Medley et al., 2020), forced by Modern-Era Retrospective analysis for Research and Applications, Version 2 (MERRA-2) climate reanalysis (Gelaro et al., 2017). Over the two-year timescale of our study, we assumed bed elevation to be constant and, thus, our surface elevation change measurements are equal to thickness change. We removed the trend from each glacier's seasonal dynamic dH, calculated over the entire duration of the available data to isolate the seasonal fluctuations from the longer-term trend. We removed 8 of the 42 glaciers with measurements of seasonal dynamic dH larger than 25m over one season, assuming that these are errors, leaving 34 glaciers for which we classified seasonal dynamic dH patterns.

https://doi.org/10.5194/tc-2021-181
Preprint. Discussion started: 14 July 2021

To account for uncertainty in seasonal dynamic dH, we propagated error through our calculations from each data source with the assumption of random, uncorrelated error. We used the error estimates provided by ATL06 to account for error on each height data point (h_sigma). Root-mean-square differences of ±8.5m between the GIMP DEM elevations and ICESat elevations were found on ice-covered terrain (Howat et al., 2014) and we assumed this to be the uncertainty on each GIMP DEM pixel's elevation value. We assume a 20% uncertainty on the thickness change due to SMB and firn components, estimated by the CFM. Assuming uncorrelated and random errors in the ATL06 and GIMP DEM surface elevation measurements, we used standard error propagation rules to calculate the error on seasonal dynamic dH, $\sigma_{s.d.dH}$:

$$\textbf{Equation 1: } \sigma_{s.d.dH} = \frac{1}{n}\left(\sum_{i=1}^{n} \sigma_{h\_li,i}^{2} + 8.5^{2}\right)^{1/2} + 0.2 \times |dH_{CFM}|$$

where $\sigma_{h\_li,i}$ represents the error on each ATL06 surface elevation measurement (h_li_sigma), 8.5 m represents the error in each GIMP DEM surface elevation, n represents the number of ATL06 elevations within the bounding box for a particular season, and dH_{CFM} is the absolute value of the magnitude of surface elevation change due to changes in SMB and firn air content changes from CFM. We do not account for uncertainty in the trend that is removed from each glacier's seasonal dynamic dH because the trend is removed solely to present the thickness changes more clearly in plots. Quantifying uncertainty in the dynamic thickness change trend could be done more thoroughly in future studies, given more ICESat-2 data that will be collected over the coming years. Additionally, keeping the trend in the seasonal dynamic dH has no impact on our categorization of glacier behavior for all but three glaciers, as we discuss in Section 4.

Using the time series of seasonal dynamic dH for each glacier, we manually grouped glaciers into categories based on their seasonal patterns of thickness change. Because seasonal dynamic dH had not been surveyed for a representative set of GrIS outlet glaciers, we did not prescribe categories prior to generating results. Instead, we based the categories on the timing of observed seasonal dynamic thinning and thickening for our surveyed glaciers. Each year of data is individually categorized; in other words, the classification for one glacier in 2019 does not influence the classification of the same glacier in 2020.

3 Results

We find that, over 2019 and 2020, the 34 surveyed glaciers can be categorized into seven seasonal patterns: no statistically significant seasonal change, mid-year thinning, mid-year thickening, spring and autumn thinning with summer thickening, summer thinning with spring and autumn thickening, sharp single season thickening, and full-year thickening (Fig. 1). Glaciers were classified into an additional category, "no statistical seasonal change," if seasonal dynamic dH uncertainties were larger than the amplitude of seasonal change across all seasons within a given year. Sharp single season thickening includes glaciers that undergo a lone season of significant (>3 times the change between any other seasons and >3 times the uncertainties for that glacier) thickening (either spring or summer) followed immediately by a similar sharp decline in thickness. Rink Isbrae is the only glacier that we identified with repeating sharp single season thickening across two years of results, undergoing 6-10m of change during this spike (Fig. 1E). Mid-year thickening refers to glaciers exhibiting two consecutive seasons of thickening

https://doi.org/10.5194/tc-2021-181
Preprint. Discussion started: 14 July 2021

in spring and summer before thinning in autumn. Conversely, mid-year thinning glaciers exhibit spring and summer thinning with thickening in autumn. Each glacier's detrended dynamic thickness change, alongside the seasonal trend of SMB and total dH change is plotted in the supplementary materials (Figs. S1 through S34). Although we have removed the trend to better illustrate seasonal dynamic dH for each glacier, we note that keeping the trend in the data does not alter our classifications for all but three glaciers: Kangerlussuup Sermia (Fig. S9), Petermann Gletsjer (Fig. S25), and Courtauld Glacier (Fig. S28). Without the trend removed from the dynamic dH, there is a slight thinning in Autumn 2020 for Petermann Gletsjer (Fig. S25). Both Kanderlussuup Sermia and Courtauld Glacier exhibit strong 1-yr trends and although there is thickening in Spring and Summer 2019 for Kangerlussuup Sermia and in Summer 2019 for Courtauld Glacier in their detrended seasonal dynamic dHs, both glaciers are actually thinning in those respective seasons without their trends removed (Figs. S9 and S28). For all other glaciers, their seasonal dynamic thickness changes are larger in magnitude than changes due to the 1- or 2-year trend and, thus, our classification is not sensitive to the removal of the trend.

We find that the 34 surveyed GrIS outlet glaciers are well distributed across the seven patterns. Figure 2 shows glacier classifications for both 2019 and 2020 in the table but displays the classification from the earliest available year on the map. With each year individually categorized, there are 47 total seasonal cycles observed between 2019 (27) and 2020 (20). Of these seasonal cycles, there are 12 seasonal cycles within the summer thinning and spring and fall thickening pattern, 10 seasonal cycles with mid-year thickening, 9 seasonal cycles exhibit summer thickening with spring and fall thinning, 6 seasonal cycles experience mid-year thinning, 3 seasonal cycles with sharp single season thickening, 1 seasonal cycle exhibiting full-year thickening, and 6 seasonal cycles with no statistical seasonal change pattern. Of the 13 glaciers for which we have two years of data, we find that most glaciers exhibit seasonal thickness change patterns that differ from year to year. Two glaciers exhibit repeating patterns: Rink Isbrae and Ussing Braer. However, the remaining glaciers for which ICESat-2 can so-far provide two annual cycles worth of data exhibit changing patterns between 2019 and 2020.

Although there are spatial clusters of glaciers with similar seasonal thickness change patterns, there is heterogeneity within the regions that contain multiple surveyed glaciers (Fig. 2). We use the 2019 classifications to compare glaciers per region because we have more glaciers classified in that year (27 glaciers). In the NW, 6 glaciers exhibit summer thinning with spring-fall thickening, 4 glaciers exhibit a mid-year thinning pattern, 2 exhibit summer thickening with spring-fall thinning, 2 exhibit mid-year thickening, and 2 exhibit no statistically significant change. In the CW, 4 glaciers exhibit summer thinning with spring-fall thickening, 3 glaciers exhibit mid-year thickening, 1 glacier exhibits sharp single season thickening, and 2 glaciers exhibit no statistically significant change. Within the SE, 3 glaciers exhibit a mid-year thickening pattern, 2 glaciers exhibit summer thickening with spring-fall thinning, and 1 glacier exhibits mid-year thinning. In the N, the single surveyed glacier, Petermann Gletsjer, exhibits summer thickening with spring-fall thinning in 2019, but notably in 2020 is the only glacier to exhibit full year thickening. Small clusters of neighboring glaciers with similar patterns can be seen in the NW (glacier IDs 29, 30, 31, 32, 34, and 40), the CW (glacier IDs 5, 6, and 8), and the SE (glacier IDs 147, 148, and 153) but there is no one pattern that is representative of all glaciers within each region.

https://doi.org/10.5194/tc-2021-181
Preprint. Discussion started: 14 July 2021

We find only a weak relationship between glacier speed and seasonal dynamic thickness change patterns. The 34 surveyed glaciers have a variety of speeds (Rignot and Mouginot, 2012; Fig. 2). The fastest glaciers in this study, with speeds above 3.5 km/yr, Kangerdlugssuaq Gletsjer (8.1 km/yr), Rink Isbrae (4.2 km/yr), and Store Gletsjer (3.71 km/yr), undergo patterns of mid-year thickening or sharp single season thickening, while medium-fast speed glaciers with speeds between 2.5 and 3.1 km/yr, such as Sermeq Kujalleq (3.1 km/yr), Kong Oscar Gletsjer (2.9 km/yr), Illullip Sermia (2.7 km/yr), and Upernavik Isstrøm S (2.5 km/yr), undergo patterns of summer or mid-year thinning. Medium-slow glaciers between 1.6 and 1.9 km/yr, such as Kangiata Nunaata Sermia (1.9 km/yr), Hayes Gletsjer (1.9 km/yr), Christian IV Gletsjer (1.8 km/yr), and Kangerlussuup Sermia (1.6 km/yr), undergo mid-year thickening. Slower glaciers, with speeds below 1.6 km/yr, are more divergent in their seasonal thickness responses, for instance Cornell Gletsjer (0.5 km/yr), Sorgenfri Gletsjer (0.3 km/yr), Sondre Parallelgletsjer (0.3 km/yr), and Courtauld Gletsjer (0.3 km/yr) are of similar speeds yet exhibit different patterns of seasonal thickness change. The slowest glacier we observe is Alangorliup Sermia (0.07 km/yr), which exhibits no statistical seasonal change in dynamic thickness.

https://doi.org/10.5194/tc-2021-181
Preprint. Discussion started: 14 July 2021

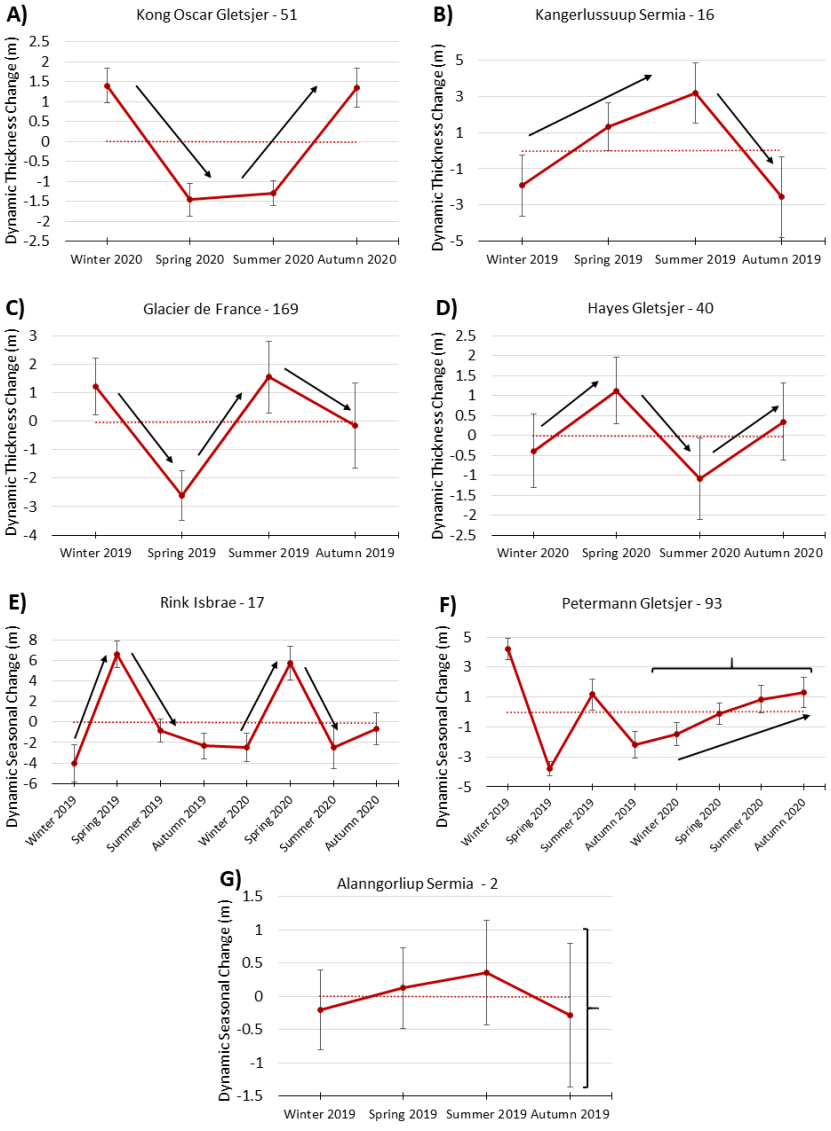

Figure 1. Patterns of outlet glacier seasonal thickness change with annual trend removed: A) mid-year thinning, B) mid-year thickening, C) spring and autumn thinning with summer thickening, D) summer thinning with spring and autumn thickening, E) sharp single season thickening, F) full-year thickening, and G) no statistically significant change. Curly brackets highlight the full-year thickening pattern of Petermann Gletsjer in 2020 (F) and the extent of the error bars encompassing no seasonal change for Alanngorliup Sermia (G).

https://doi.org/10.5194/tc-2021-181
Preprint. Discussion started: 14 July 2021

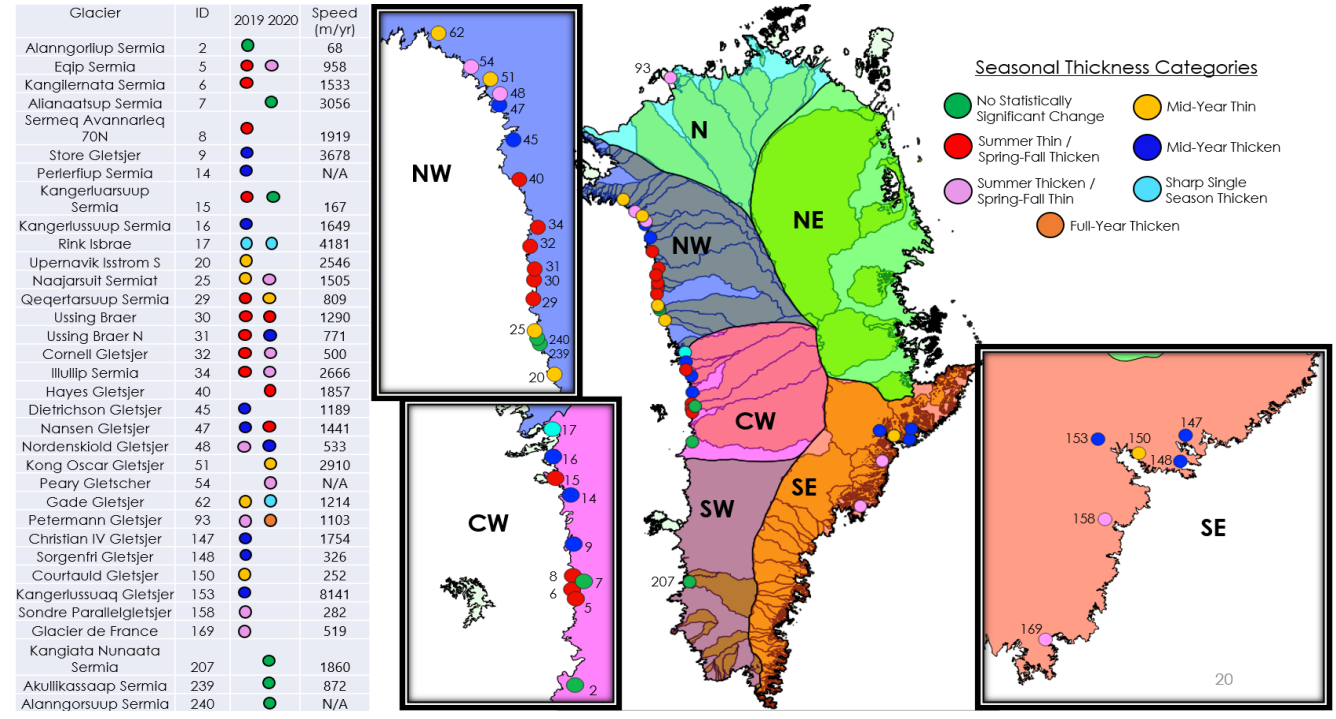

Figure 2. Locations, seasonal dynamic thickness change patterns, and average ice speeds of 34 GrIS outlet glaciers. Glaciers with different patterns in 2019 and 2020 are depicted on the ice sheet map with their 2019 pattern coloration, while both 2019 and 2020 patterns are shown in yearly pattern left-side table. Speed is given for glaciers, based on data available in Rignot and Mouginot, 2012.

4 Discussion and conclusions

Enabled by 91-day repeat measurements from ICESat-2, we have developed the first classification of GrIS outlet glacier seasonal dynamic thickness change patterns for a representative sample of glaciers from around the ice sheet. We have chosen to use the ATL06 data product and to account for along- and across-track surface slopes using the GIMP DEM as a reference elevation dataset. This method allowed us to aggregate surface elevation data within customized bounding boxes, representative of each glacier's behavior. Higher-level data products, such as ATL11 and ATL15, will provide estimates of surface elevation change through time and we believe it will be worthwhile for future work to compare our results against the higher-level ICESat-2 products, both to build confidence in our results and as a check on the data products themselves.

Our results reveal little regional coherency in seasonal dynamic thickness change patterns, indicating that atmospheric circulation patterns are not the likely driver of differences in patterns among glaciers. While we do find small clusters of similar patterns, we do not observe similar patterns across larger ice sheet regions. If atmospheric forcing were the primary driver of seasonal dynamic thickness changes, we would expect to see coherent patterns of seasonal changes across each region. However, we do not find this to be the case, indicating that other factors that differ from glacier to glacier within each region

https://doi.org/10.5194/tc-2021-181
Preprint. Discussion started: 14 July 2021

are causing the differences in observed patterns. This finding is consistent with seasonal glacier velocity changes, which also exhibit spatial heterogeneity (Moon et al., 2014; Vijay et al. 2019). Ocean forcing may be responsible for the differences in seasonal dynamic thickness change patterns because heat transport from the continental shelf to the termini of outlet glaciers is modulated by fjord geometry, which is heterogeneous among glaciers (Carroll et al., 2017). Each glacier's unique geometry, which has been shown to govern observed differences in terminus retreat (Catania et al., 2018) and the multi-annual upstream diffusion of thinning (Felikson et al., 2021), may also be responsible for the observed heterogeneity in seasonal thickness changes.

Refining the ATL06 data quality flag (atl06_quality_summary), with the goal of accepting additional good-quality measurements that are currently flagged as poor-quality, would benefit future studies of seasonal outlet glacier change. Because ICESat-2 has a repeat cycle of 91 days, collecting good-quality data from each pass is critical to studies of the seasonal thickness changes of outlet glaciers. The current set of parameters used by the ATL06 quality summary flag may remove good-quality measurements over rough topography, high surface slopes, or low-reflectivity surfaces under clouds (Smith et al., 2021). In the course of our study, we found that 12 additional glaciers, of the subset of 65 glaciers we initially selected from the MEaSUREs dataset, could be included in our results, had we ignored the quality summary flag entirely. Of course, some of the measurements that are removed by the quality summary flag are unusable and we do not advocate ignoring data quality checks entirely. However, we suggest that further inspection of the parameters used for the quality summary flag to potentially reduce the strictness by which data is eliminated may prove useful and would allow additional glaciers to be considered.

As ICESat-2 continues data collection, future work should build on our two-year assessment of seasonal dynamic thickness changes by extending our record and comparing with other glacier variables and external forcings. The MEaSUREs dataset identifies 239 total outlet glaciers around the ice sheet and, by adding more outlet glaciers and extending the record forward in time, future studies can examine how consistent the patterns are from year to year, identify new patterns not exhibited by the glaciers in our study, and better identify glaciers that exhibit the same or different patterns through time. With a longer and more comprehensive classification of seasonal thickness changes, future work can focus on compiling a holistic record of seasonal glacier dynamics by investigating thickness changes together with terminus position and velocity changes. The subset of glaciers that we have selected for study are ones that have a temporally rich dataset of terminus position changes from the newly developed CALFIN automated deep learning extraction method (Cheng et al., 2020) allowing our results to be directly compared with seasonal terminus positions. Finally, to advance our understanding of the processes that drive seasonal glacier behavior, future work should compare seasonal dynamic thickness changes with external forcings such as seasonal ocean temperature changes and surface meltwater runoff estimates. Our study provides the first classification of seasonal dynamic thickness changes of outlet glaciers around the GrIS to complement previous classifications of seasonal velocity change (Moon et al., 2014; Vijay et al. 2019), bringing us one step closer to a holistic understanding of seasonal glacier dynamics.

https://doi.org/10.5194/tc-2021-181
Preprint. Discussion started: 14 July 2021

Author contribution. C.T. and D.F. conceptualized the experiment and goals. C.T. carried out the experiment, developed the code, and performed the simulations. C.T. prepared the manuscript with written review and editing from D.F and T.N. T.N. performed project administration and funding acquisition.

Data and code availability. The Supplementary Information associated with this brief communication contains the seasonal thickness change measurements presented in the manuscript, along with the surface mass balance component of seasonal thickness change from the Community Firn Model and MERRA-2. Additionally, a shapefile of locations of the glaciers surveyed is provided.

Competing interests. There are no competing interests to disclose about this brief communication.

Acknowledgements. This work was performed through the NASA Goddard Space Flight Center Internship Program, administered by the Goddard Space Flight Center Office of Education and funded by the ICESat-2 Project Science Office. Resources supporting this work were provided by the NASA High-End Computing (HEC) Program through the NASA Center for Climate Simulation (NCCS) at the Goddard Space Flight Center. We thank Brooke Medley for providing output from the Community Firn Model.

References

Carroll, D., Sutherland, D. A., Shroyer, E. L., Nash, J. D., Catania, G. A., & Stearns, L. A.: Subglacial discharge-driven renewal of tidewater glacier fjords, Journal of Geophysical Research: Oceans, 125(9), 2293. http://doi.org/10.1002/grl.50825, 2017.

Catania, G. A., Stearns, L. A., Sutherland, D. A., Fried, M. J., Bartholomaus, T. C., Morlighem, M., Shroyer, E., Nash, J.: Geometric Controls on Tidewater Glacier Retreat in Central Western Greenland. Journal of Geophysical Research: Earth Surface, 29(1), 1–15, http://doi.org/10.1029/2017JF004499, 2018.

Cheng, D., Hayes, W., Larour, E., Mohajerani, Y., Wood, M., Velicogna, I., and Rignot, E.: Calving Front Machine (CALFIN): Glacial Termini Dataset and Automated Deep Learning Extraction Method for Greenland, 1972–2019, The Cryosphere Discuss. [preprint], https://doi.org/10.5194/tc-2020-231, in review, 2020.

Choi, Y., Morlighem, M., Rignot, E., Wood, M.: Ice dynamics will remain a primary driver of Greenland ice sheet mass loss over the next century, Communications Earth & Environment 2, 26, https://doi.org/10.1038/s43247-021-00092-z, 2021

Church, J.A., Clark, P.U., Cazenave, A., Gregory, J.M., Jevrejeva, S., Levermann, A., Merrifield, M.A., Milne, G.A., Nerem, R.S., Nunn, P.D., Payne, A.J., Pfeffer, W.T., Stammer, D., and Unnikrishnan, A.S.: Sea Level Change. In Climate Change 2013: The Physical Science Basis. Contribution of Working Group I to the Fifth Assessment Report of the Intergovernmental Panel on Climate Change [Stocker, T.F., Qin, D., Plattner, G.-K., Tignor M., Allen, S.K., Boshung, J., Nauels, A., Xia, Y., Bex, V., and Midgley, P.M., (eds.)], Cambridge University Press, Cambridge, United Kingdom and New York, NY, USA. http://doi.org/10.1017/CBO9781107415324.026, 2013.

Felikson, D., Catania, G. A., Bartholomaus, T. C., Morlighem, M., & Noël, B. P. Y.: Steep Glacier Bed Knickpoints Mitigate Inland Thinning in Greenland, Geophysical Research Letters, 48(2), e2020GL090112, http://doi.org/10.1029/2020GL090112, 2021.

Gelaro, R., McCarty, W., Suárez, M. J., Todling, R., Molod, A., Takacs, L., Randles, C. A., Darmenov, A., Bosilovich, M. G., Reichle, R., Wargan, K., Coy, L., Cullather, R., Draper, C., Akella, S., Buchard, V., Conaty, A., da Silva, A. M., Gu, W., Kim, G., Koster, R., Lucchesi, R., Merkova, D., Nielsen, J. E., Partyka, G., Pawson, S., Putman, W., Rienecker, M., Schubert, S. D., Sienkiewicz, M., & Zhao, B.: The Modern-Era Retrospective Analysis for Research and Applications, Version 2 (MERRA-2), *Journal of Climate*, *30*(14), 5419-5454, https://journals.ametsoc.org/view/journals/clim/30/14/jcli-d-16-0758.1.xml, 2017.

Howat, I., Negrete, A., and Smith, B.: The Greenland Ice Mapping Project (GIMP) land classification and surface elevation data sets, The Cryosphere. 8, 1509-1518, https://doi.org/10.5194/tc-8-1509-2014, 2014.

Joughin, I., Moon, T., Joughin, J., and Black, T.: MEaSUREs Annual Greenland Outlet Glacier Terminus Positions from SAR Mosaics, Version 1. Boulder, Colorado USA. NASA National Snow and Ice Data Center Distributed Active Archive Center. https://doi.org/10.5067/DC0MLBOCL3EL, 2015, 2017.

Markus, T., Neumann, T., Martino, A., Abdalati, W., Brunt, K., Csatho, B., Farrell, S., Fricker, H., Gardner, A., Harding, D., Jasinski, M., Kwok, R., Magruder, L., Lubin, D., Luthcke, S., Morison, J., Nelson, R., Neuenschwander, A., Palm, S., Popescu, S., Shum, CK., Schutz, B., Smith, B., Yang, Y., Zwally, J.: The Ice, Cloud, and land Elevation Satellite-2 (ICESat-2): Science requirements, concept, and implementation. Remote Sens. Environ., Vol 190, 2017, pp. 260-273, ISSN 0034-4257, https://doi.org/10.1016/j.rse.2016.12.029, 2017.

Medley, B., Neumann, T., Zwally, H. J., and Smith, B. E.: Forty-Year Simulations of Firn Processes over the Greenland and Antarctic Ice Sheets, The Cryosphere Discussions, vol. 2020, 2020, pp. 1–35, https://doi.org/10.5194/tc-2020-266, 2020.

Moon, T., Joughin, I., Smith, B., van den Broeke, M. R., van de Berg, W. J., Noël, B., and Usher, M.: Distinct patterns of seasonal Greenland glacier velocity, Geophys. Res. Lett.,41, 7209–7216, https://doi.org/10.1002/2014GL061836, 2014.

Mouginot, J., Rignot, E., Bjørk, A., van den Broeke, M., Millan, R., Morlighem, M., Noël, B., Scheuchl, B., and Wood, M.: Forty-Six Years of Greenland Ice Sheet Mass Balance from 1972 to 2018, Proceedings of the National Academy of Sciences, vol. 116, no. 19, p. 9239, doi:10.1073/pnas.1904242116, 2019.

Neumann, T. A., Martino, A. J., Markus, T., Bae, S., Bock, M.R., Brenner, A. C., Brunt, K. M., Cavanaugh, J., Fernandes, S.T., Hancock, D. W., Harbeck, K., Lee, J., Kurtz, N. T., Luers,P. J., Luthcke, S. B., Magruder, L., Pennington, T. A., Ramos-Izquierdo, L., Rebold, T., Skoog, J., and Thomas, T. C.: The Ice,Cloud, and Land Elevation Satellite – 2 mission: A global geolo-cated photon product derived from the Advanced Topographic Laser Altimeter System, Remote Sens. Environ., 233, 111325,https://doi.org/10.1016/j.rse.2019.111325, 2019.

Oppenheimer, M., Glavovic, B. C., Hinkel, J., van de Wal, R., Magnan, A. K., Abd-Elgawad, A., Cai, R., Cifuentes-Jara, M., DeConto, R. M., Ghosh, T., Hay, J., Isla, F., Marzeion, B., Meyssignac, B., and Sebesvari, Z.: Sea Level Rise and Implications for Low-Lying Islands, Coasts and Communities. In: IPCC Special Report on the Ocean and Cryosphere in a Changing Climate [H.-O. Pörtner, D.C. Roberts, V. Masson-Delmotte, P. Zhai, M. Tignor, E. Poloczanska, K. Mintenbeck, A. Alegría, M. Nicolai, A. Okem, J. Petzold, B. Rama, N.M. Weyer (eds.)], IPCC Special Report on the Ocean and Cryosphere in a Changing Climate, 126. (In Press), https://www.ipcc.ch/site/assets/uploads/sites/3/2019/11/08_SROCC_Ch04_FINAL.pdf, 2019.

Rignot, E., Mouginot, J.: Ice flow in Greenland for the International Polar Year 2008-2009, Geophysical Research Letters, 39 (11), art. no. L11501, https://doi.org/10.1029/2012GL051634, 2012.

Shepherd, A., Ivins, E., Aa, G., & Barletta, V., Bentley, M., Bettadpur, S., Briggs, K., Bromwich, D., Forsberg, R., Galin, N., Horwath, M., Jacobs, S., Joughin, I., King, M., Lenaerts, J., Li, J., Ligtenberg, S., Luckman, A., Luthcke, S., and Zwally, H.: A Reconciled Estimate of Ice-Sheet Mass Balance, Science, Vol 338, Issue 6111, pp. 1183-1189. https://doi.org/ 10.1126/science.1228102, 2012.

Smith, B., Fricker, H. A., Holschuh, N., Gardner, A. S., Adusumilli, S., Brunt, K. M., Csatho, B., Harbeck, K., Huth, A., Neumann, T., Nilsson, J., and Siegfried, M. R.: Land Ice Height-Retrieval Algorithm for NASA's ICESat-2 Photon-Counting Laser Altimeter, Remote Sensing of Environment, vol. 233, 2019, p. 111352, https://doi.org/10.1016/j.rse.2019.111352, 2019.

Smith, B., Fricker, H. A., Gardner, A., Siegfried, M. R., Adusumilli, S., Csathó, B. M., Holschuh, N., Nilsson, J., Paolo, F. S., and the ICESat-2 Science Team.: ATLAS/ICESat-2 L3A Land Ice Height, Version 3, Boulder, Colorado USA, NASA National Snow and Ice Data Center Distributed Active Archive Center, https://doi.org/10.5067/ATLAS/ATL06.003, 2020.

Smith, B.E., Harbeck, K., Roberts, L., Neumann, T., Brunt, K., Fricker, H.A., Gardner, A., Seigfried, M.R., Adusumilli, S., Csatho, B.M., Holschuh, N., Nilsson, J., Paolo, F.S.: ICESat-2 Algorithm Theoretical Basis Document (ATBD) for Land Ice Along- Track Height (ATL06), Applied Physics Laboratory, University of Washington, Seattle, WA available at. https://icesat-2.gsfc.nasa.gov/science/data-products, 2021.

Vijay, S., Khan, S. A., Kusk, A., Solgaard, A. M., Moon, T., & Bjørk, A. A.: Resolving Seasonal Ice Velocity of 45 Greenlandic Glaciers With Very High Temporal Details, Geophysical Research Letters, 46(3), 1485–1495, http://doi.org/10.1029/2018GL081503, 2019.